

Sensor Technology Limited

P O Box 97, 20 Stewart Road
Collingwood, Ontario, Canada L9Y 3Z4
E-Mail: Techsupport@sensortech.ca
World Wide Web: www.sensortech.ca

Tel: 705.444.1440
Fax: 705.444.6787



**An Experimental Investigation of Vibration Suppression of a
Flexible Cantilever Beam via Linear coupling Control**

Phil Salemi

April 1995

**AN
EXPERIMENTAL INVESTIGATION
OF
VIBRATION SUPPRESSION
OF A FLEXIBLE
CANTILEVER BEAM
VIA LINEAR COUPLING
CONTROL**

Prepared for:

**Prof. M. F. Golnaraghi
Prof. G. R. Heppler**

**Dr. E. Prasad
BM HiTech
Collingwood, Ontario**

**Phil Salemi
Mechanical Engineering
University of Waterloo**

April 1995

TABLE OF CONTENTS

SUMMARY.....	3
CONCLUSIONS.....	4
1.0 Introduction.....	5
1.1 Linear Coupling Background.....	7
1.2 Linear Controller Development.....	9
1.2.1 Linear Controller Theory.....	9
1.2.2 Linear Coupled Controller Circuit.....	13
2.0 Experimental Apparatus.....	17
2.1 Experimental Procedure.....	19
3.0 Experimental Results.....	20
3.1 Beam Initial Position 29 mm.....	20
3.1.1 Vary Controller Frequency and Damping.....	21
3.1.2 Vary Controller Initial Condition.....	26
3.1.3 Vary Controller Disable Time.....	28
3.2 Beam Initial Position 11 mm.....	30
3.3 Velocity Feedback Controller.....	32
4.0 Adaptation to Digital Control.....	33
REFERENCES.....	34

LIST OF FIGURES

Figure 1: Cantilever Beam With Slider Mechanism.....	5
Figure 2: Beam with Rotor Arm Mechanism	6
Figure 3: Beam with Piezoelectric Actuators	6
Figure 4: Double Pendulum with Linear Spring	7
Figure 5: Double Pendulum Response	8
Figure 6: State Diagram of Damped Harmonic Oscillator.....	9
Figure 7: Coupled Plant and Controller.....	11
Figure 8: Plant and Controller State Diagram.....	12
Figure 9: Integration Op-Amp Circuit.....	13
Figure 10: Variable Gain Op-Amp Circuits.....	14
Figure 11: Summing and Inverting Op-Amp.....	14
Figure 12: LC Controller Analog Circuit.....	15
Figure 13: Cantilever Beam.....	17
Figure 14: Cantilever Beam and Control System	18
Figure 15: 29 mm Uncontrolled Response	20
Figure 16: Plant and Controller Response $\omega=16.3$ rad/s and $\zeta=0.05$	21
Figure 17: Plant Response $\omega=16.3$ rad/s and $\zeta=0.09$	23
Figure 18: Plant Response $\omega=15.5$ rad/s and $\zeta=0.05$	23
Figure 19: Plant Response $\omega=17.6$ rad/s and $\zeta=0.05$	25
Figure 20: Plant Response $\omega=16.3$ rad/s and $\zeta=0.07$	26
Figure 21: Plant Response $\omega=16.3$ rad/s and $\zeta=0.07$ and IC=1V.....	27
Figure 22: Plant Response $\omega=16.3$ rad/s and $\zeta=0.07$ and IC=2.5V.....	27
Figure 23: Plant Response $\omega=16.3$ rad/s and $\zeta=0.05$ and IC=6V and $\tau_d=.878$	28
Figure 24: Plant Response $\omega=16.3$ rad/s and $\zeta=0.05$ and IC=6V and $\tau_d=.756$	29
Figure 25: 11 mm Uncontrolled Response	30
Figure 26: Plant Response $\omega=19$ rad/s and $\zeta=0.3$ and IC=6V	30
Figure 27: Plant Response $\omega=16.3$ rad/s and $\zeta=0.03$ and IC=6V and $\tau_d=.706$	31
Figure 28: 29 mm with State Feedback Controller.....	32

SUMMARY

This report is presented as an experimental study of the control of a flexible cantilever beam by means of piezoceramic actuators and a Linear Co-ordinate Coupling controller using analog circuitry. The theory for the controller is explained via an intuitive double pendulum analogy demonstrating how energy may be extracted from a plant and eliminated in a coupled linear system. The development continues with an overview of the control block diagram and its electrical equivalents in the analog circuit. A description of migrating the controller to an analog/digital hybrid is also included.

The experimental apparatus is described and schematics of its components are given, the beam employed is an 18 inch long, 1 inch wide, .03 inch thick aluminum cantilever beam. The experiment was run from two different initial tip deflections 11 mm and 29 mm under different control conditions, that is, uncontrolled, varying controller frequency, varying controller damping, varying controller initial conditions, and varying controller disable time. Time responses of the acceleration of the plant are shown for each control condition.

The results of the laboratory experiment demonstrate the efficacy of the LC controller on small and large oscillations. Time responses for the controlled cases showed that vibration due to initial condition could be quelled on the order of 1 to 1.5 seconds, compared to greater than 45 seconds uncontrolled. The results are compared with previous experiments with a velocity state feedback controller, and it is observed that the LC controller outperforms in terms of immediate response. However, the state feedback controller is more robust to random inputs, where as the LC controller works only under preset initial conditions. Methods for overcoming the LC controller's limitations are discussed by means of adaptation of a digital computer in combination with the analog circuit.

CONCLUSIONS

The result of the laboratory experiments show a significant improvement in the decay time for the controlled beam over the uncontrolled response. From the 29 mm initial deflection the controller is able to damp the response in less than 1.5 seconds, without control the response takes over 45 seconds to settle. The 11 mm initial condition is controlled in approximately one second.

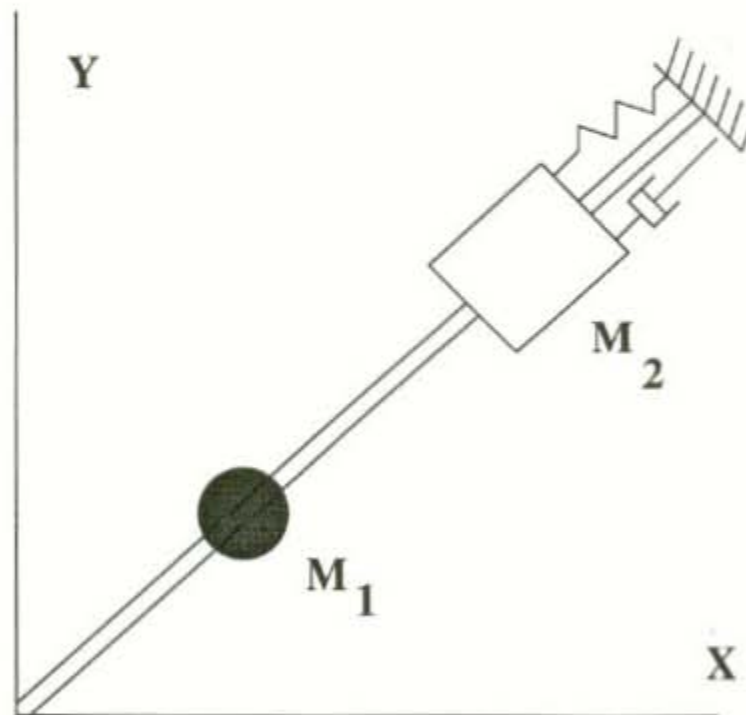
The experiments also demonstrate the various relationships between controller frequency and damping settings. By increasing the controller frequency it is possible to reduce the response time of the plant, however stability is affected. Controller initial conditions were also demonstrated to improve plant response by further minimizing the energy in the plant at disable time.

1.0 Introduction

Recently, due to greater requirements in space applications, flexible structures have undergone an increased amount of research. Due to these structure's low mass, small stiffness, and the environmental characteristics of a vacuum they tend to have little structural damping. Therefore, they are significantly affected by disturbances from orbital maneuvers and impacts [1].

These characteristics require sophisticated control strategies in order to reduce and eliminate vibration. Several control methods have been attempted. Golnaraghi has introduced an active/passive system to regulate vibration in a cantilever beam by means of nonlinear coupling [2]. The essence of the method relies on the addition of spring-mass-dashpot mechanism to the cantilever beam, see Figure 1, basically adding a degree of freedom to the system. Due to the coupling between the beam and the second mass there is an energy exchange between the modes. This may be exploited as a means to extract energy from the system by dampening it when it is in the secondary mode, thus suppressing vibration in the beam. The key lies in the fact that the energy in the beam itself cannot be damped, however, once in the secondary mode it may be terminated.

Figure 1: Cantilever Beam With Slider Mechanism



This secondary mechanism has been successfully implemented experimentally as a rotating moment arm rigidly fixed to a servo motor [3], see Figure 2. The net effect of the mechanism is that of a singular moment of varying amplitude applied at the end of the beam. A similar means of applying a moment to the beam is with piezoelectric crystal couples acting as actuators. The piezoelectric phenomenon is exhibited by materials that

become electrically charged when stressed, or conversely, undergo mechanical deformation when an electrical field is applied [4]. Thus the current research in control of flexible structures involves the use of piezoelectric materials as actuators. For the cantilever beam they need not only be applied to the end, but potentially anywhere along the beam, see Figure 3.

Figure 2: Beam with Rotor Arm Mechanism

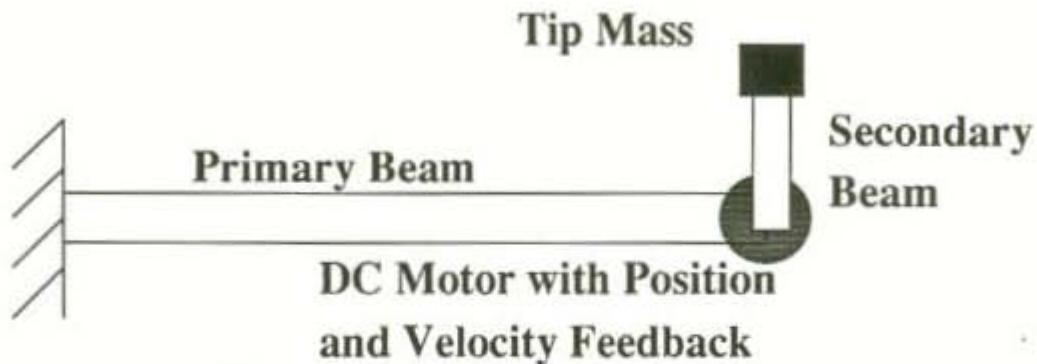
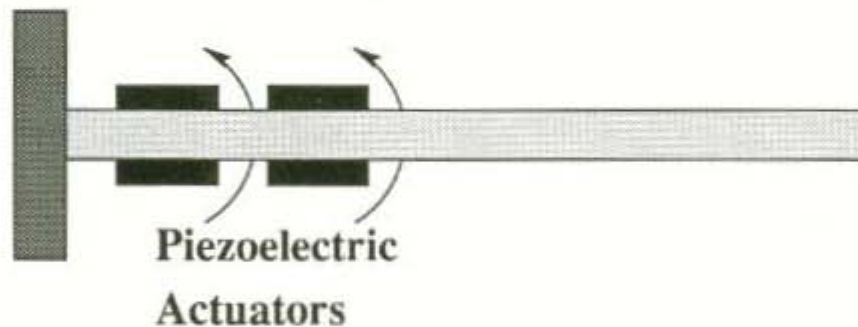


Figure 3: Beam with Piezoelectric Actuators

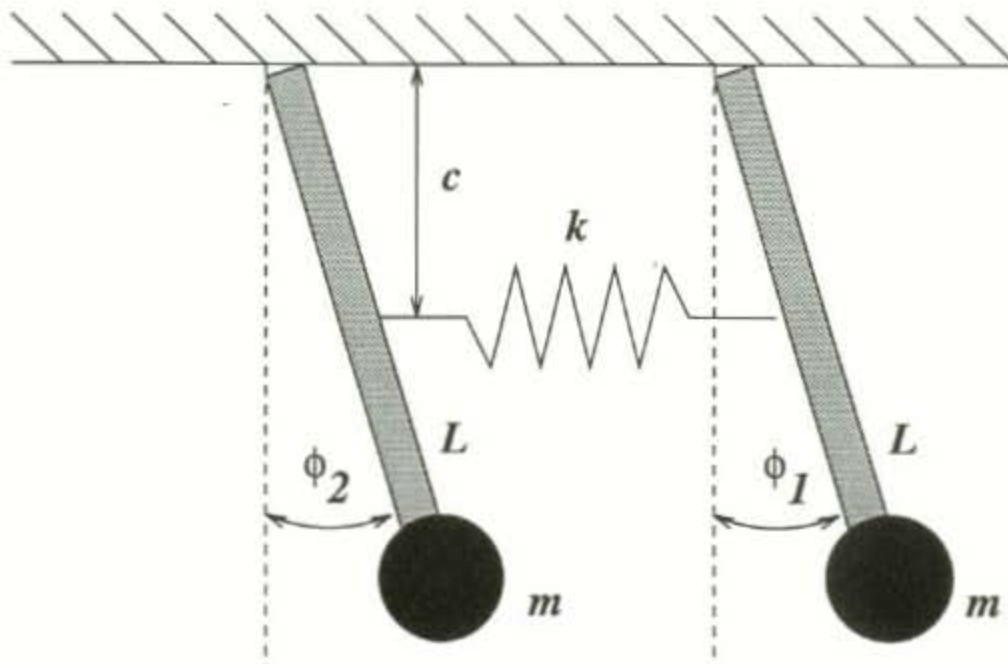


The purpose of this experimental investigation is to determine the feasibility and effectiveness of a novel control strategy for vibration suppression in a cantilever beam. The control strategy to be implemented is an energy exchange method where energy is extracted and dissipated from the beam via linear coupling to a secondary system. In this case the secondary system, or controller, is a single degree of freedom linear oscillator that has been emulated with linear electronic circuitry. The effect of the controller is actuated upon the beam via piezoceramic elements bonded to the beam.

1.1 Linear Coupling Background

The essence of this control technique relies upon an exchange of energy from the primary mode, that is the beam, and a secondary mode, the LC controller. This method has been employed traditionally as method of vibration absorption in mechanical systems with forced oscillations Inman [5]. In this case a second mass-spring system is added to the primary system, thus changing from a single degree of freedom to a two degree of freedom. The system now has two natural frequencies, and the secondary one may be tuned such that the amplitude of the primary mode is minimized. This notion of augmenting the order of the system may be observed more intuitively in the double pendulum model. Here two identical pendulums are joined by a linear spring as shown in Figure 4.

Figure 4: Double Pendulum with Linear Spring



The linearized equations of motion are derived by Thomson [6] and shown to be:

$$\begin{aligned} mL^2\ddot{\phi}_1 + mgL\phi_1 + Kc^2(\phi_1 - \phi_2) &= 0 \\ mL^2\ddot{\phi}_2 + mgL\phi_2 - Kc^2(\phi_1 - \phi_2) &= 0 \end{aligned}$$

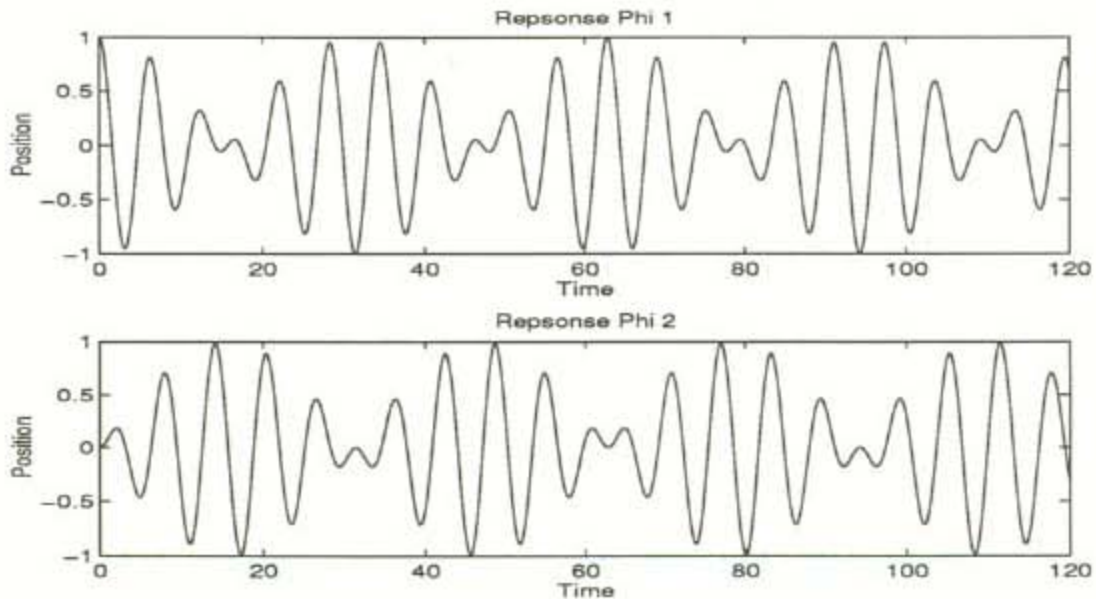
It is observed from these equations that there is a linear coupling term in each, in other words the Φ_2 in the first equation and the Φ_1 in the second. Assuming that link 1 is given an initial displacement and link 2 is initial at rest the solution to these governing equations will be:

$$\phi_1(t) = \phi_0 \cos\left(\frac{\omega_b - \omega_a}{2} t\right) \cos\left(\frac{\omega_b + \omega_a}{2} t\right)$$

$$\phi_2(t) = \phi_0 \sin\left(\frac{\omega_b - \omega_a}{2} t\right) \sin\left(\frac{\omega_b + \omega_a}{2} t\right)$$

These equations are illustrated in Figure 5, it is observed that when one co-ordinate reaches an energy maximum that the other is at an energy minimum. It is this energy transfer which is to be exploited in the LC controller, such that the link is severed when the primary co-ordinate reaches a minimum, thus suppressing the vibration.

Figure 5: Double Pendulum Response



Thus, in the case of controlling a flexible structure such as a cantilever beam it is possible to model the controller as a second order linear oscillator, and the beam as the primary co-ordinate.

1.2 Linear Controller Development

The previously described double pendulum analogy may be extended to the coupling of co-ordinates between any two linear harmonic oscillators. In each case a primary co-ordinate may be defined as the plant which is to be regulated and the secondary co-ordinate may be defined as the controller which will transfer energy from the plant.

1.2.1 Linear Controller Theory

The controller has been defined as a virtual version of a simple linear harmonic oscillator with a tunable natural frequency and variable damping. The most general expression for such a system is:

$$M\ddot{x} + C\dot{x} + Kx = 0$$

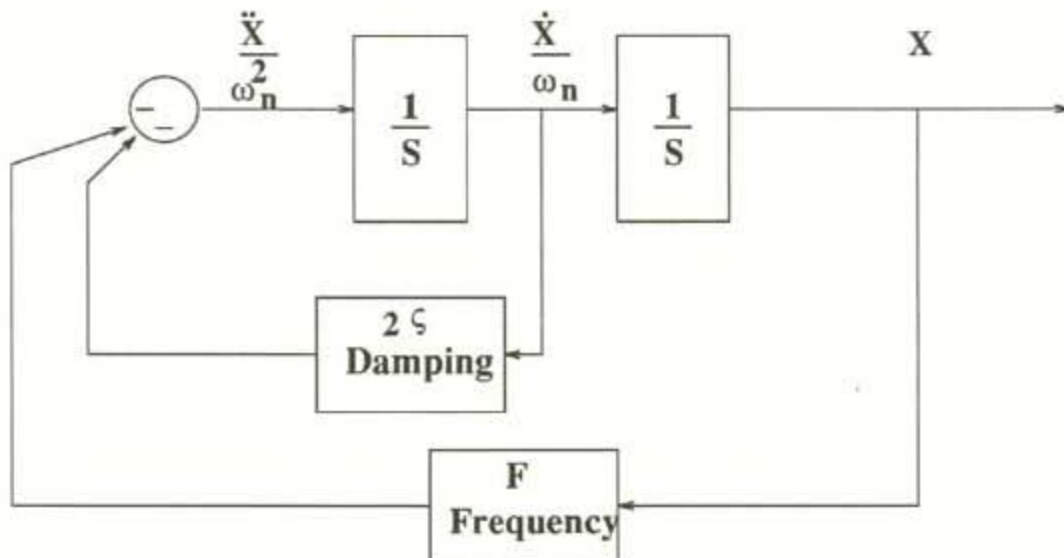
or

$$\ddot{x} + 2\zeta\omega_n\dot{x} + \omega_n^2x = 0$$

This may be re-expressed in terms of a summation of state variables which may be subsequently illustrated by means of a state diagram or block diagram in Figure 6.

$$\frac{\ddot{x}}{\omega_n^2} = -\left(\frac{2\zeta\dot{x}}{\omega_n} + x\right)$$

Figure 6: State Diagram of Damped Harmonic Oscillator



The frequency of the oscillator may be varied by adding a variable gain in the feedback term from x to the comparator, allowing the natural frequency to be multiplied by a constant proportional to ω_n . The damping may be varied by also making the damping feedback a variable gain. This results in a fully tunable second order system with all states defined.

Both the plant and controller equations may now be expressed in a form including coupling terms which force each co-ordinate independently. The coupling terms are defined as single linear states of the other co-ordinate.

The general equation for the plant is:

$$\ddot{x}_p + 2\zeta\omega_p\dot{x}_p + \omega_p^2x_p = G_1u(\ddot{x}_c, \dot{x}_c, x_c)$$

The general equation for the controller is:

$$\ddot{x}_c + 2\zeta\omega_c\dot{x}_c + \omega_c^2x_c = G_2y(\ddot{x}_p, \dot{x}_p, x_p)$$

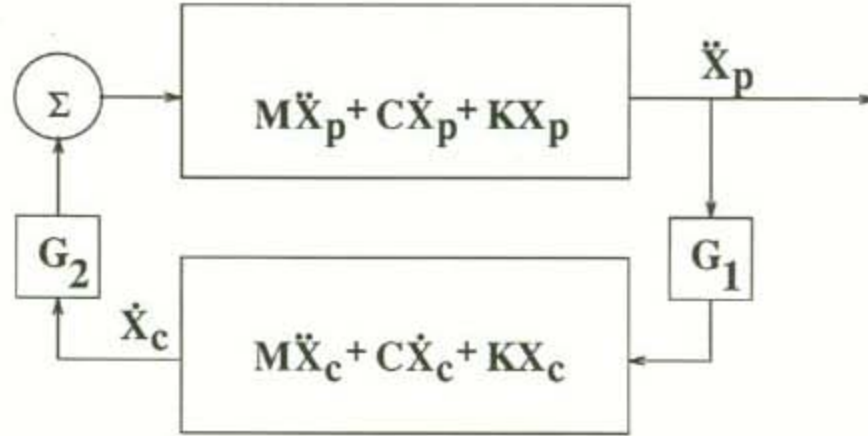
Thus the coupling term u may be defined as either: \ddot{x}_c, \dot{x}_c , or x_c and the coupling term y may be defined as either \ddot{x}_p, \dot{x}_p , or x_p . The states that are finally implemented were chosen via trial and error in the laboratory. The criteria by which this was decided is two fold, firstly the combination had to produce a beating phenomenon between the primary and secondary co-ordinates. Secondly, the beats had to have a short period with a clearly defined minimum. The experimentally determined states to produce this were: $u = \dot{x}_c$ and $y = \ddot{x}_p$. Thus the state equations are finally defined as:

$$\ddot{x}_p + 2\zeta\omega_p\dot{x}_p + \omega_p^2x_p = G_1\dot{x}_c$$

$$\ddot{x}_c + 2\zeta\omega_c\dot{x}_c + \omega_c^2x_c = G_2\ddot{x}_p$$

This system of equations may be shown in block diagram as in Figure 7.

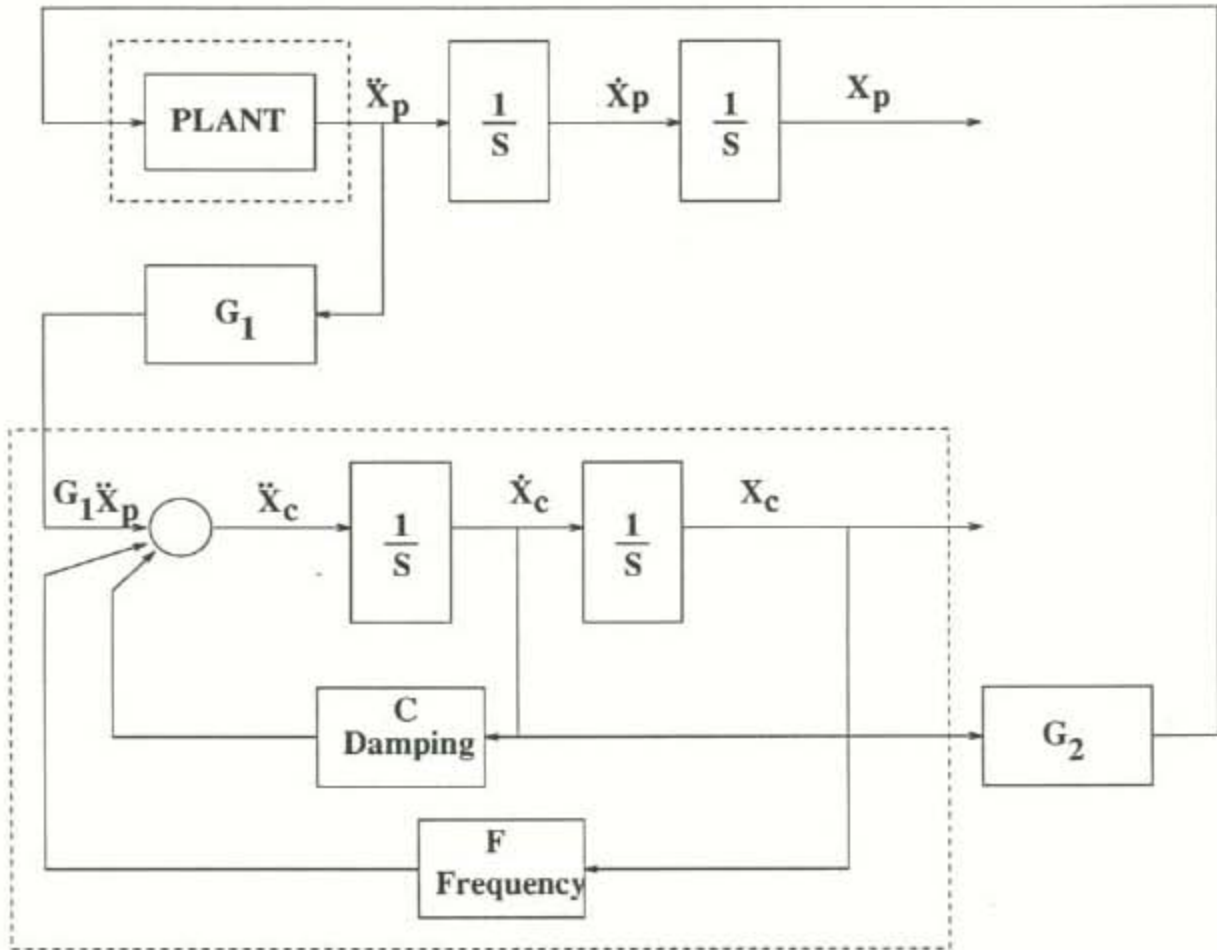
Figure 7: Coupled Plant and Controller



This block diagram may be augmented to include the previous block diagram for the controller shown in Figure 6. It is necessary to include the coupling gains of G_1 and G_2 such that their contribution to the energy exchange may be varied. The result is the configuration shown in Figure 8.

The controller has a damping gain C which is equivalent to 2ζ in Figure 6, and a frequency gain F which is a variable gain which manipulates the controllers natural frequency. Here, the output of the controller is the same as has been defined previously and shown in Figure 7 as $G_2\dot{x}_c$. However, either of the other two states of the controller may be used, but this yielded the best result. Furthermore, since the plant consists of a beam with a tip accelerometer and it is desired to have all the states of the plant defined, integration was performed twice on the accelerometer signal. This allowed the possibility of trying all plant and controller state combinations.

Figure 8: Plant and Controller State Diagram

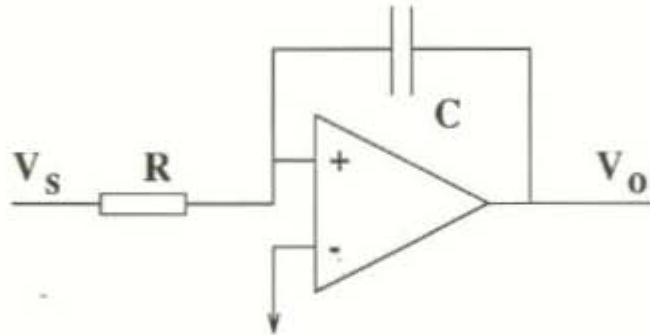


The system has been defined mathematically and may be implemented by a number of means including analog circuitry, or digital computer.

1.2.2 Linear Coupled Controller Circuit

The outlined LC controller can be implemented as other compensators either analog or digital, however analog circuitry is selected for its versatility and processing time. The block diagram consists only of integrations and variable or constant gains, these are realized via operational amplifiers configured for each function. The integration operation is represented by the equivalent circuit shown in Figure 9.

Figure 9: Integration Op-Amp Circuit



The transfer function for this circuit is:

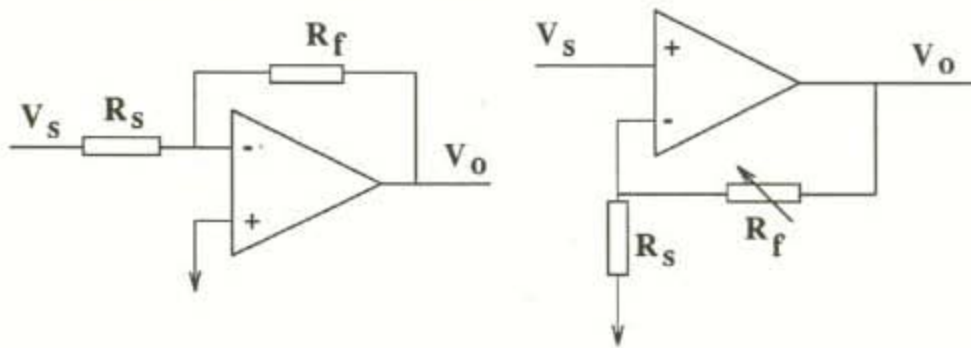
$$v_o(t) = -\frac{1}{RC} \int v_i(t) dt$$

Hence, the gain of the integrator is $-1/RC$ and therefore results in an inversion and integration. The RC chosen for the experiment is 0.1 yielding a net op-amp gain of -10 per integrator, thus two integrators in series yield a gain of 100. By recalling the state diagram shown in Figure 4, this means that the base natural frequency of the controller is 10 rad/s. Adding a gain F to the loop feedback results in a natural frequency for the controller of

$$\omega_c = 10\sqrt{F}$$

The gains may be either inverting or non-inverting, and constant or variable. The following circuits in Figure 10 represent variable inverting amplifier on the left and a variable non-inverting amplifier on the right.

Figure 10: Variable Gain Op-Amp Circuits



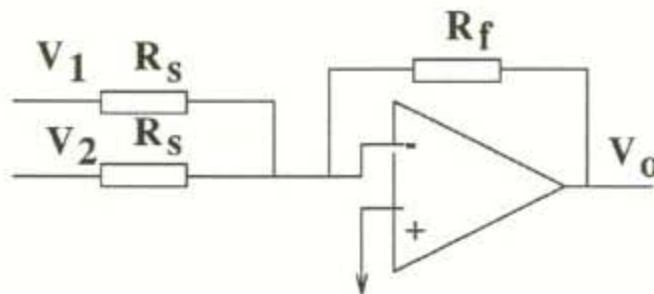
The transfer function for these circuits are as follows:

$$v_o = -\frac{R_f}{R_s} v_s \quad v_o = \frac{R_f + R_s}{R_s} v_s$$

The gain of the damping constant C uses an inverting variable gain amplifier such that the damping ratio is expressed by $\zeta = C/2$.

The comparator that is necessary to sum all the feedback signals as shown in Figure 4 is done with a summing and inverting op-amp shown in Figure 11:

Figure 11: Summing and Inverting Op-Amp

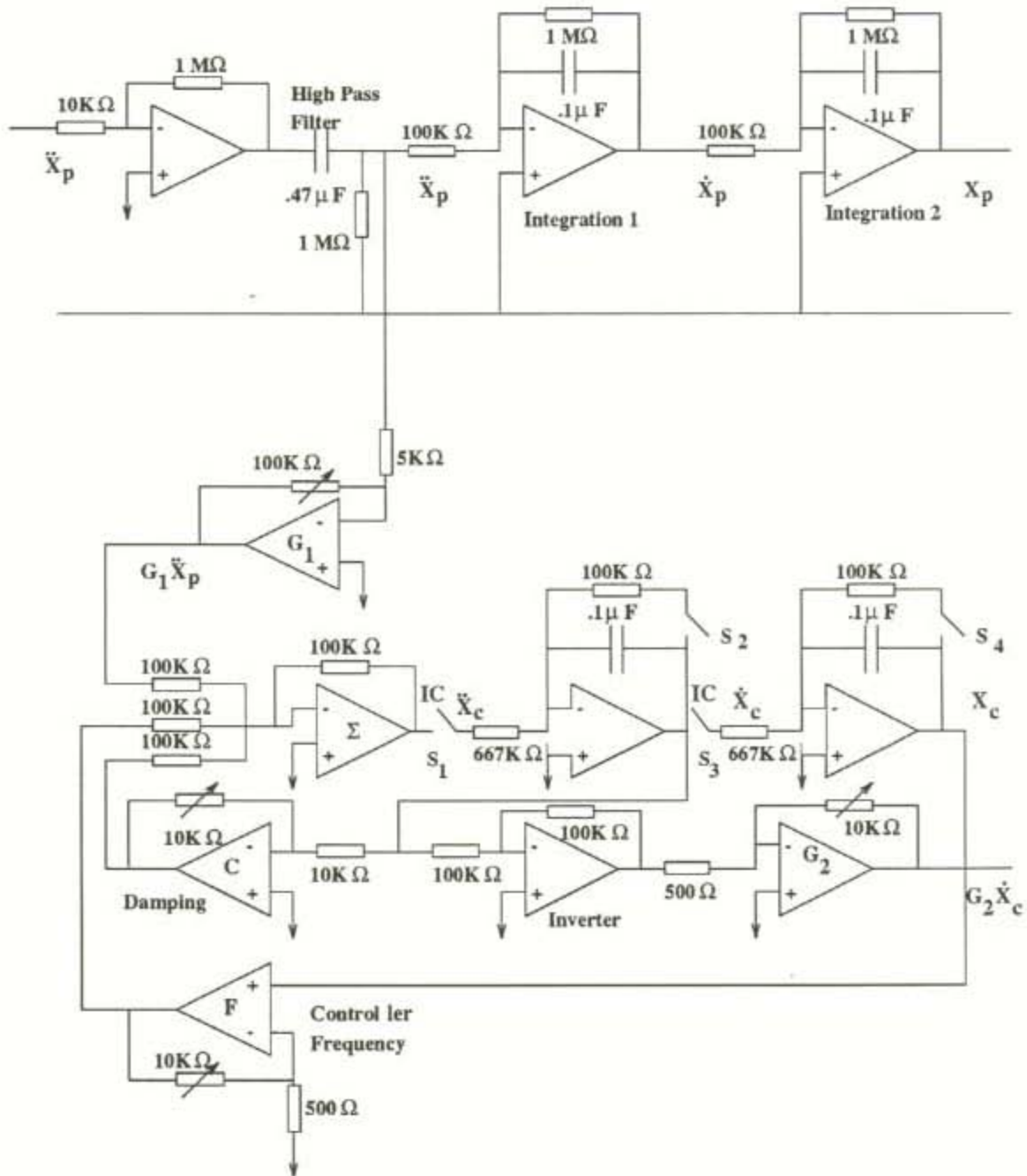


The transfer function of the circuit is:

$$v_o = -(v_1 + v_2) \frac{R_f}{R_s}$$

The basic components of a the controller circuit have been defined and may be substituted according to the block diagram in Figure 6. The circuit diagram in Figure 12 is the analog equivalent of the linear coupled controller, and operates entirely in low voltages with ± 15 V supply. The gains for frequency F and damping C are set with potentiometers and the summation is accomplished with the summing and inverting amplifier with a gain of unity.

Figure 12: LC Controller Analog Circuit



The controller also requires some signal conditioning, thus the input signal from the accelerometer is first amplified by a $\times 100$ inverting op-amp, and then high pass filtered in order to remove DC offset. This signal is then used as the input to the controller circuit via an inverting op-amp with transfer function of $G_1\ddot{x}_p$. The output of the controller is taken from the $-\dot{x}_c$ node, recall that the integrators invert the signal. The controller velocity is inverted again with a gain of unity and then amplified to give an output signal of $G_2\dot{x}_c$.

The initial condition for velocity and position of the controller were imposed by having S_1 and S_3 initially open and connected to a voltage proportional to the initial condition. Switches S_2 and S_4 are initially closed such that they limit the charge to the capacitors. When the beam is released a switch is triggered to a relay such that all the switches change states and the loop is closed.

Finally, the output of the controller to the HVPS is lead through a timing disable circuit. This circuit will cut the signal to the controller after a set time of operation. This serves the purpose of disabling output to the beam at the instant of an energy minimum in the plant. The time must be preset by the operator using the observation of when the plant reaches a minimum with out the disable.

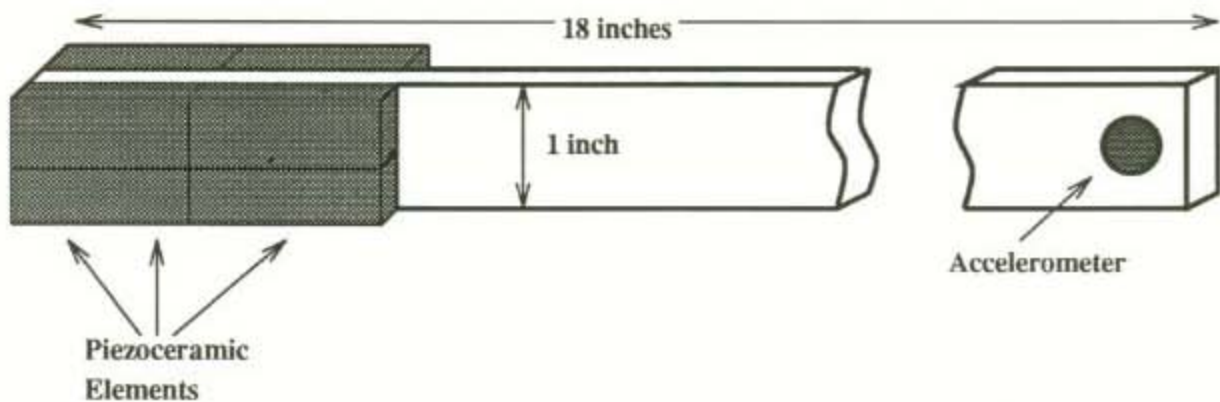
Thus the controller has been fully developed and defined in analog circuitry. Now this circuit must be connected with the acceleration source signal and the High Voltage Power Amplifier (HVPS) that drives the piezoceramic elements.

2.0 Experimental Apparatus

The plant the controller is implemented on, as mentioned in the Introduction, is a cantilever beam rigidly clamped with a C clamp at its base. The base is rigidly affixed to an aluminum test bed which is 18x18 inches. Hence, the beam is sufficiently isolated from any extraneous vibrations. The beam shown in Figure 13 has the following characteristics:

Material	Aluminum 6061-T6
Density	2770 kg/m³
Length	18 inches (457.2 mm)
Width	1 inch (25.4 mm)
Thickness	.030 inch (.76 mm)

Figure 13: Cantilever Beam

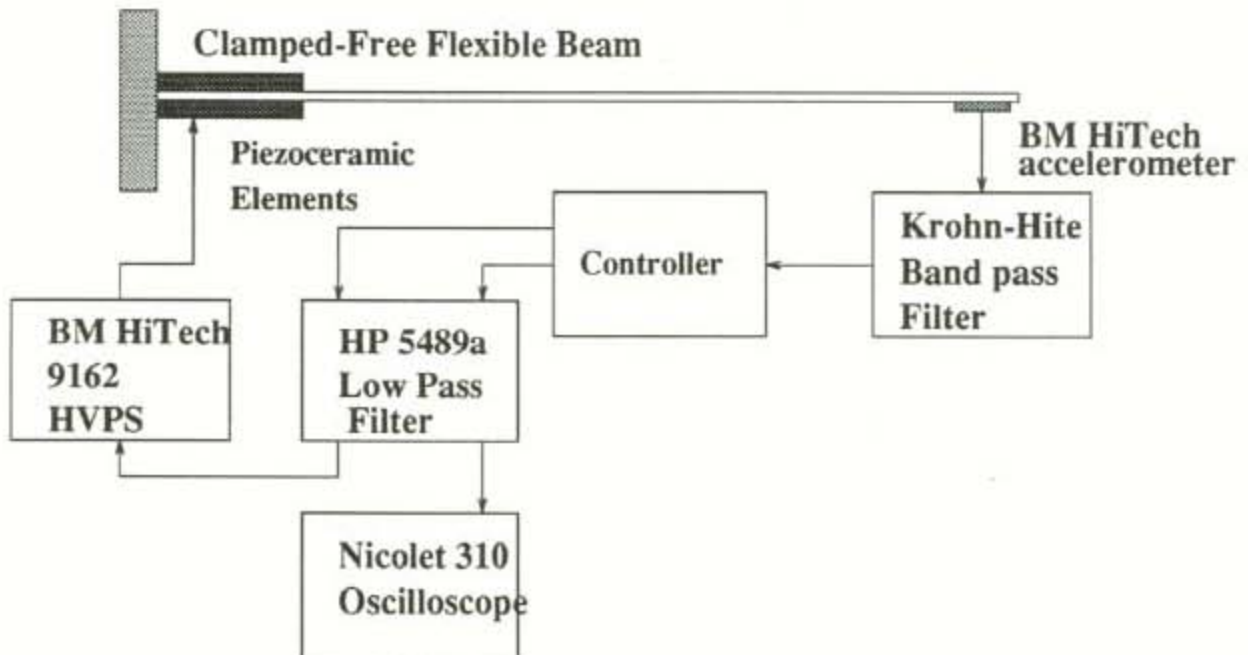


The piezoceramics are bonded to the aluminum beam with a proprietary epoxy made by BM-HiTech. The actuators are made of material BM532, for which pertinent properties are listed below, and are arranged in banks of 4 elements per side, starting at the clamped base. They are bonded such that dielectric pole are all pointed in the same direction, and when soldered the positive lead is joined to all the sides facing outward from the beam. The negative lead is bonded to the substructure, as the epoxy is sufficiently conductive to permit current to flow to the sides facing the substructure. Hence, the same alternating signal can drive both banks of piezos at 180° out of phase.

Young's Modulus (E_a)	71E9 N/m²
Density (ρ_a)	7350 kg/M³
Charge Constant (d_{31})	2.00E-10 m/V

The sensor employed is a BM HiTech accelerometer placed at the tip of the cantilever beam. The wires from the accelerometer are taped for most of the length of the beam and then suspend in order to eliminate any contribution to damping. The acceleration is filtered and fed to an analog circuit which pre-amplifies, and integrates the signal twice such that acceleration, velocity, and position are all known. As shown in Section 1.2.1 a plant signal, acceleration, is used to force the controller, and an output from the controller, velocity, is used in turn to force the plant. Each of these signals are filtered before being applied to the next stage. The feedback signal is once again amplified by a high voltage amplifier and used to excite the piezoceramic actuators, see Figure 14.

Figure 14: Cantilever Beam and Control System



2.1 Experimental Procedure

The test bed platform is installed with a release mechanism for the beam tip such that a reproducible initial condition may be used. A switch is located adjacent to the release mechanism which triggers the relays that are part of the circuit when the beam is released. The gain of the 9162 HVPS is set to maximum, and the "sensor" input is shorted, and the DC offset is set so that no clipping results in the HVPS output. Hence, the only way to vary the gain is by changing the feedback potentiometer in the output of the controller G_2 .

The input and output parameters G_1 and G_2 were determined by examining the open loop. By setting G_1 first such that a sufficient gain would cause the controller output to beat and then setting G_2 such that the output of the HVPS did not clip when the beam was at maximum amplitude and required maximum feedback voltage to the piezos.

Once those parameters were set, the remaining parameters are the frequency gain F , the damping gain C , the initial conditions for velocity and position (IC1 and IC2 respectively), and the disable time T . These parameters are varied by the following method:

- 1) The frequency and damping are varied until the most well defined beat phenomenon is observed.
- 2) Then the initial position is varied with initial velocity set to zero (initial velocity was not varied as there is a high pass filter eliminating offset in the HVPS, hence any initial condition for $G_2\dot{x}_c$ will immediately be negated), this results in an improvement in the first minimum such that it is closer to zero.
- 3) Finally, the disable time is varied so that the output is cut when the beam is at a minimum energy.

The initial conditions used are 29 mm and 11 mm initial tip deflection.

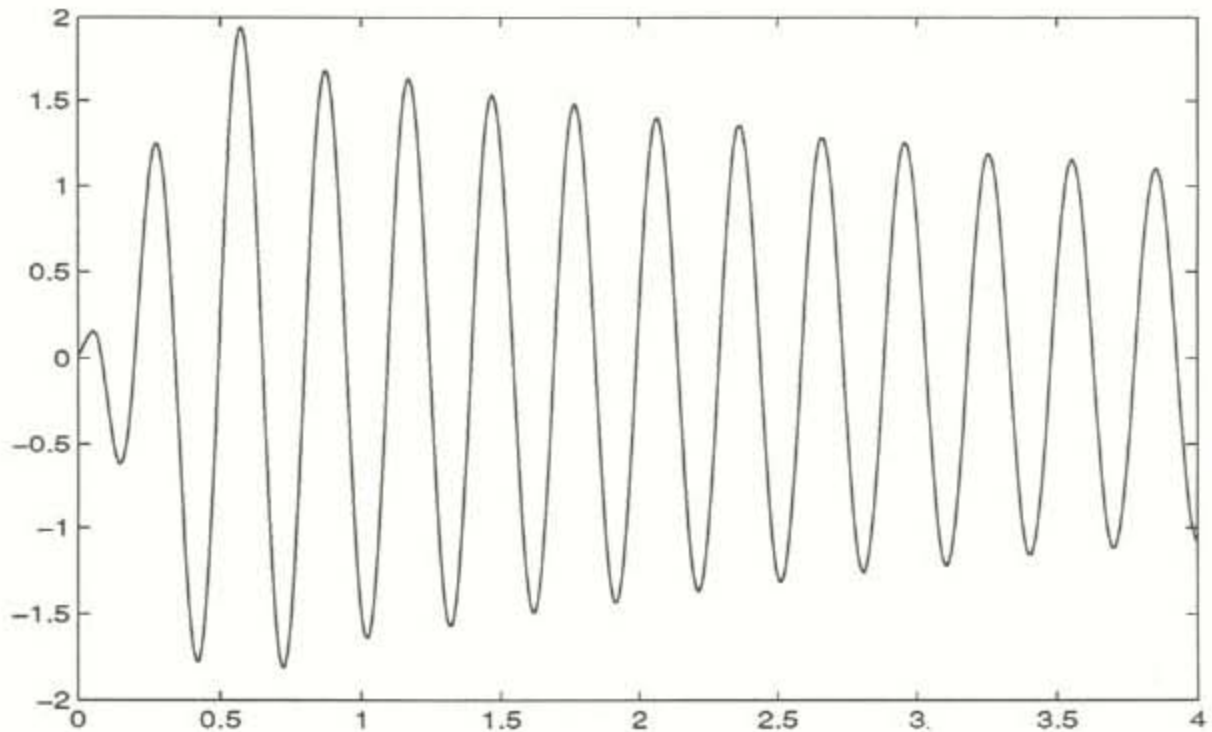
3.0 Experimental Results

The results of the procedure previously outlined are presented in the form of the response of the plant acceleration, hence, they all begin at the origin. First, the results of the 29 mm initial tip deflection are presented, the results for the 11 mm initial condition are shown. For the 29 mm IC the complete development of the ideal control parameters is shown, however for the 11 mm IC only the final step of tuning the disable time is shown.

3.1 Beam Initial Position 29 mm

Without any control action the response from this initial condition will dampen out due to inherent structural damping in the material in greater than 45 seconds. The uncontrolled response is shown in Figure 15.

Figure 15: 29 mm Uncontrolled Response

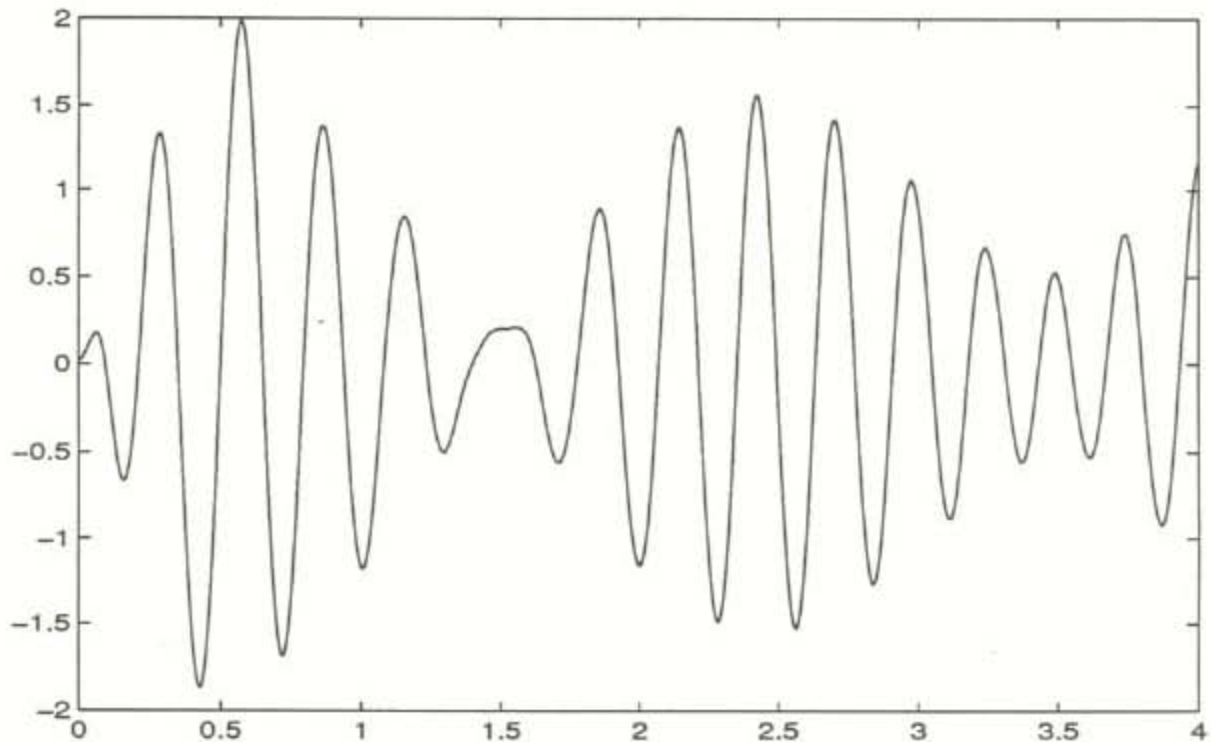


3.1.1 Vary Controller Frequency and Damping

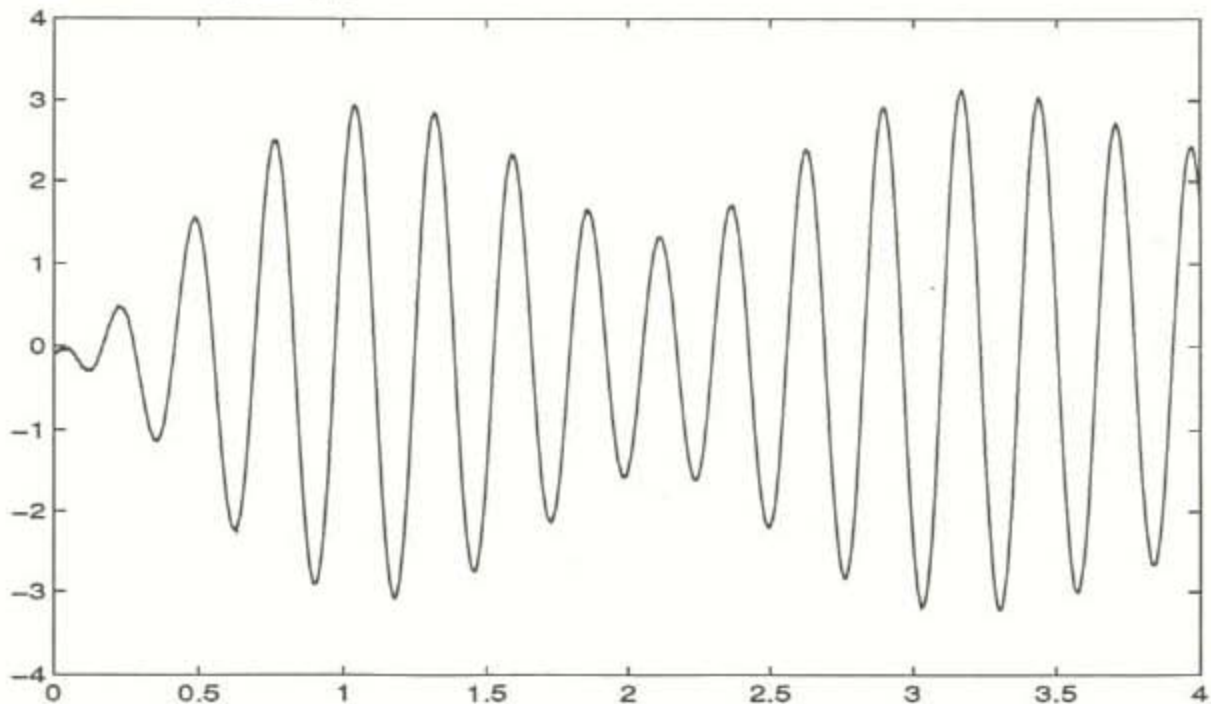
The LC controller is initially set to nominal frequency and damping values and then fine tuned. Initially the controller is set to $\omega=16.3$ rad/s and $\zeta=0.05$. The response of the plant, shown as $G_1\ddot{x}_p$, and the response of the controller is shown as $G_2\dot{x}_c$ in Figure 16. It is clear from the figure that these show a definite out-of-phase coupling where the energy in the controller is maximized when the energy in the plant is minimized.

Figure 16: Plant and Controller Response $\omega=16.3$ rad/s and $\zeta=0.05$

Plant Output $G_1\ddot{x}_p$:

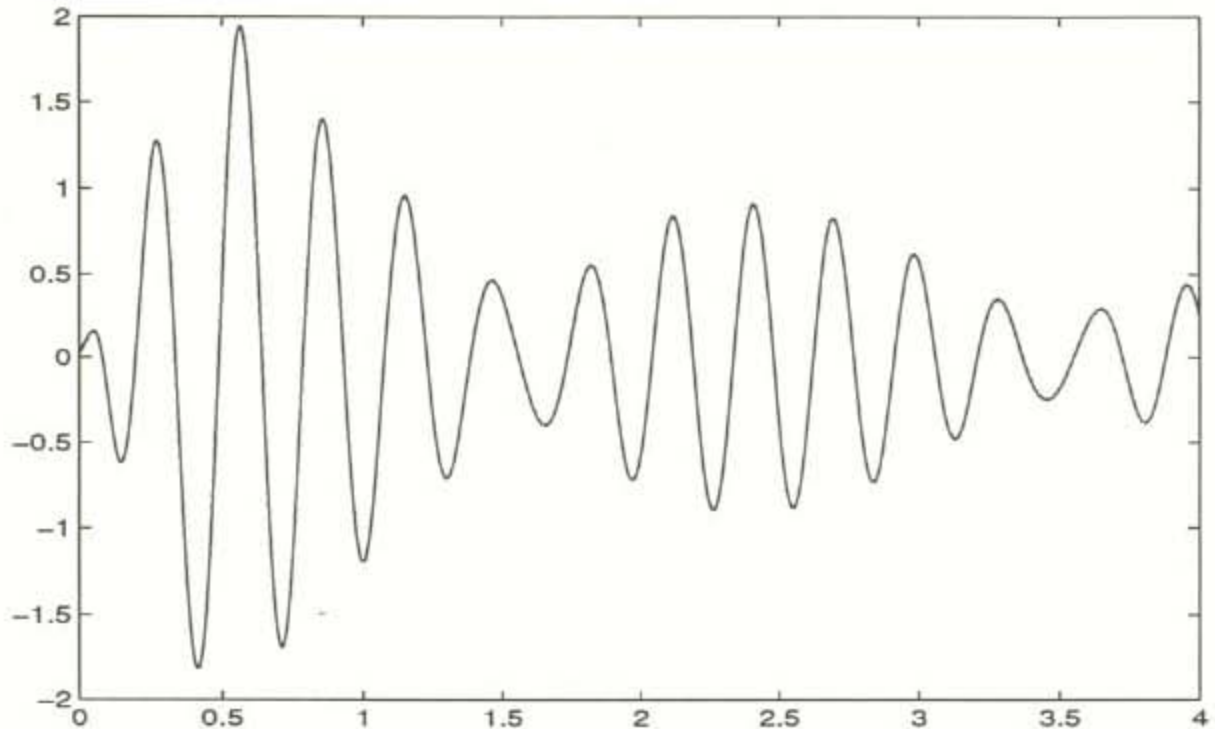


Controller Output $G_2\dot{x}_c$



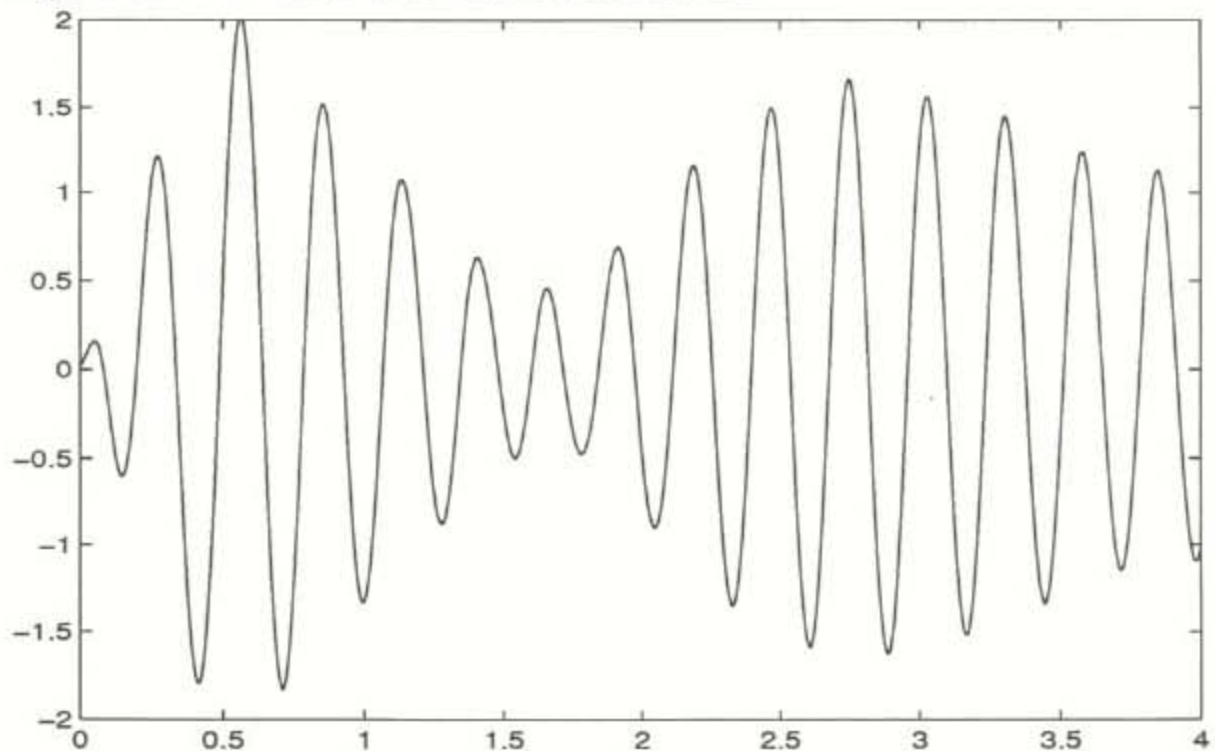
By varying the damping co-efficient of the controller, in this case increasing the damping to $\zeta=0.09$ and keeping the frequency constant at $\omega=16.3$ rad/s the response of the plant shows that less energy is returned, see Figure 17.

Figure 17: Plant Response $\omega=16.3$ rad/s and $\zeta=0.09$



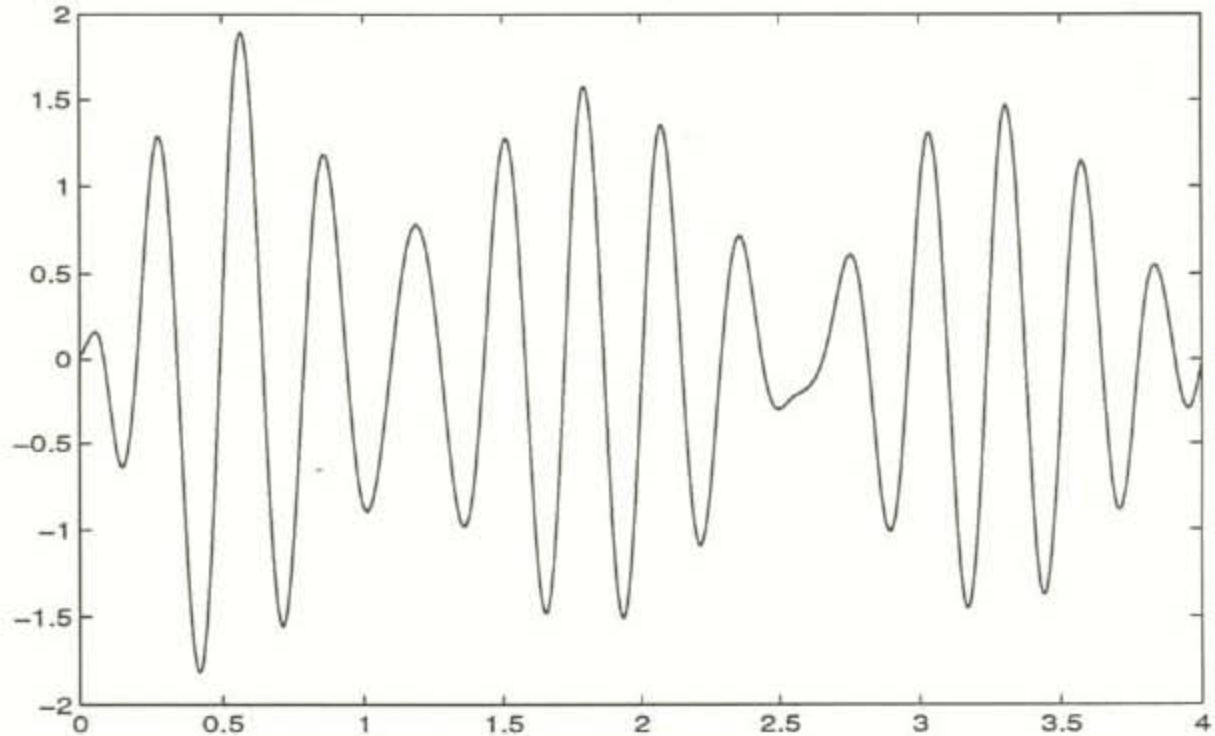
However, by decreasing the frequency of the controller, ie changing the beat frequency between the co-ordinates, it is possible to change the time to the first minimum. With $\omega=15.5$ rad/s and damping held constant at $\zeta=0.05$, the response shown in Figure 18 shows an increase in the time to first minimum.

Figure 18: Plant Response $\omega=15.5$ rad/s and $\zeta=0.05$



An increase in the controller frequency to $\omega=17.6$ rad/s and damping kept the same results in an increase in the beat frequency between co-ordinates, and thus significantly reduces the time for first minimum, see Figure 19.

Figure 19: Plant Response $\omega=17.6$ rad/s and $\zeta=0.05$



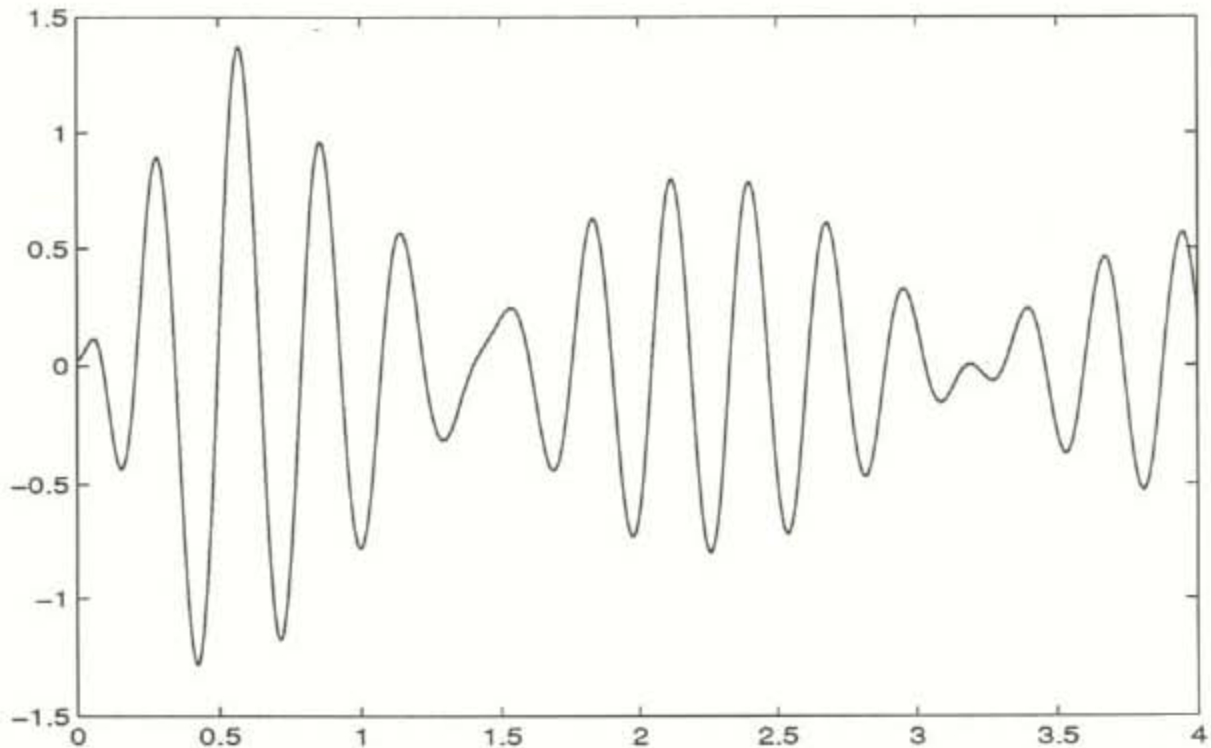
It is clear from these responses that varying frequency and damping in the controller significantly alters the response of the plant. However, obtaining a first minimum with the lowest possible energy is not completely possible by setting only these parameters. The lowest possible energy in the minimum is desirable in that the disabling of the controller output will result in a zero energy remaining in the plant. For example, if the disable were initiated at the first minimum in the above figure, the result would be remnant oscillations in the plant.

3.1.2 Vary Controller Initial Condition

By changing the initial condition in the controller it is possible to effect a different output in the plant. This simply translates into starting the controller in a higher energy state, thus beginning the control with a greater compensation signal. For this experiment only initial position is varied in the controller and is measured in volts. Initial velocity was not possible to implement because the output of the controller is its velocity signal, and this is filtered with a high pass filter after the HVPS to remove steady state offset. Hence, any initial velocity is immediately filtered.

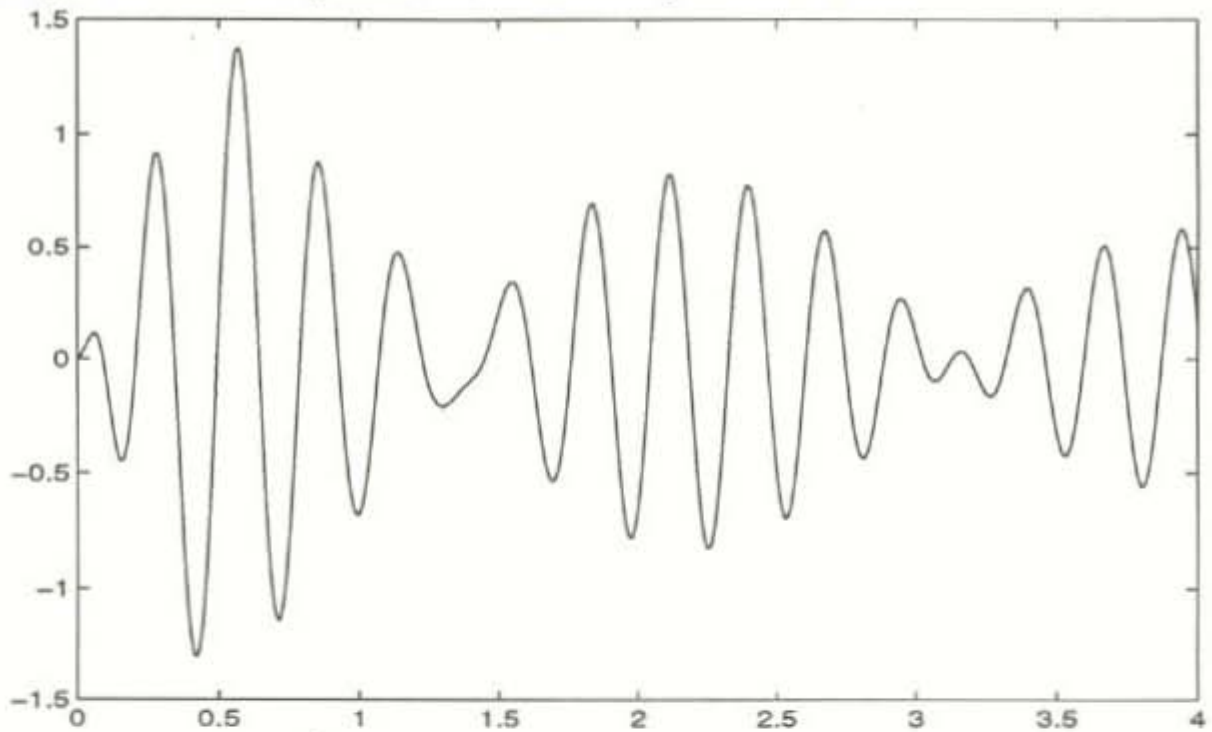
The first attempt is with no initial condition and the frequency set for $\omega=16.3$ rad/s and damping set for $\zeta=0.07$, see Figure 20. This results in a first minimum around 1.4 seconds, however, it is still somewhat large in amplitude and it is desirable to reduce.

Figure 20: Plant Response $\omega=16.3$ rad/s and $\zeta=0.07$



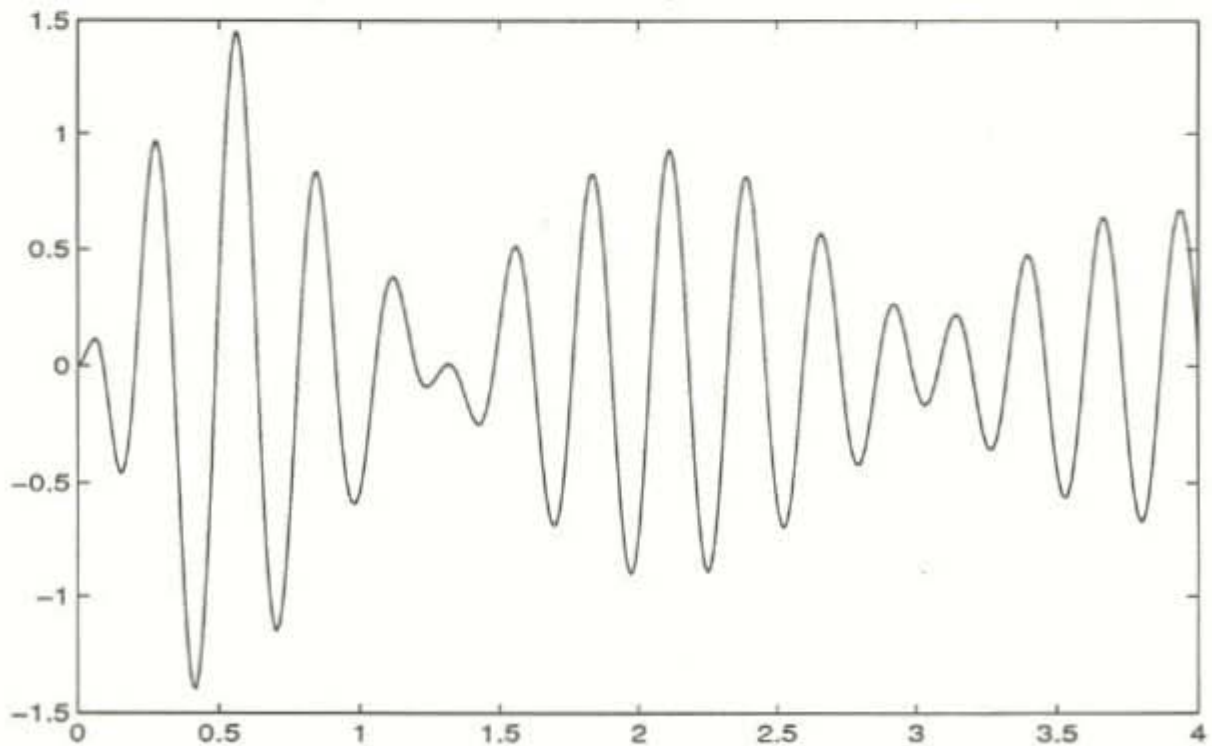
We increase the initial condition of the controller to 1 V and the response shown in Figure 21 becomes a little flatter at the 1.3 second point.

Figure 21: Plant Response $\omega=16.3$ rad/s and $\zeta=0.07$ and IC=1V



A more improved response results from an IC of 2.5 V. Here the energy minimum level is nearly zero and may be disabled with very little remnant oscillations, see Figure 22.

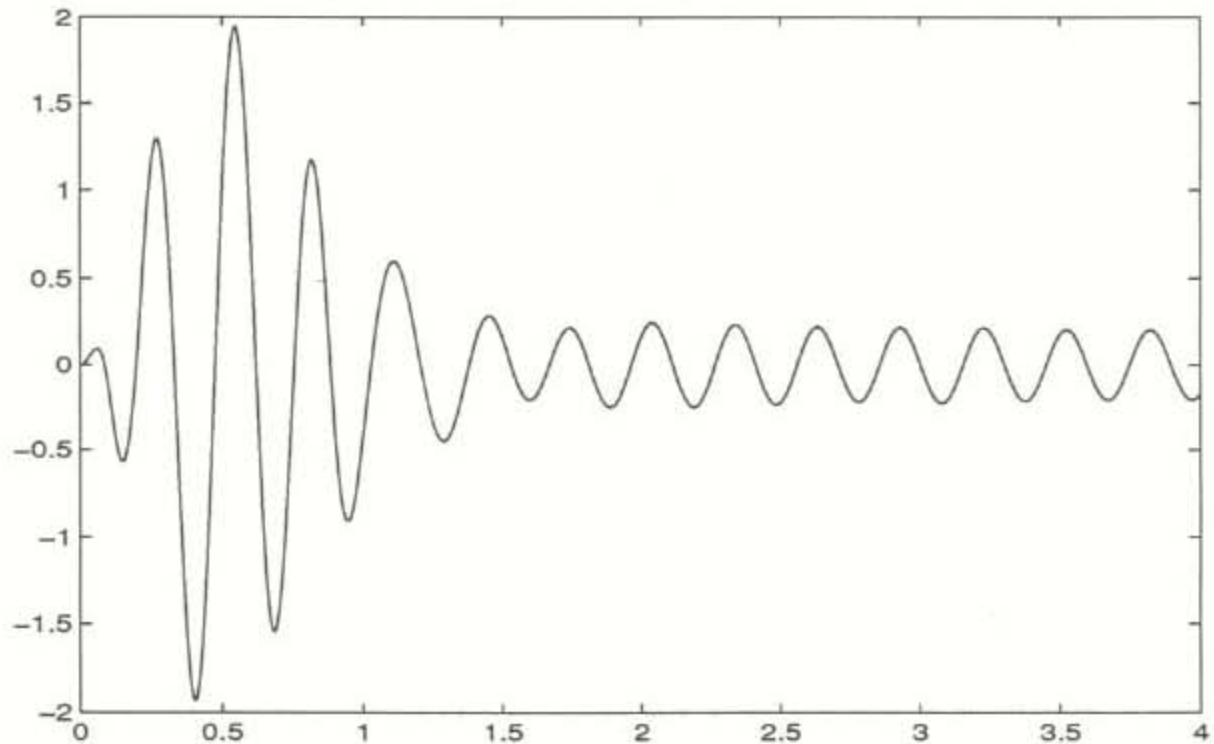
Figure 22: Plant Response $\omega=16.3$ rad/s and $\zeta=0.07$ and IC=2.5V



3.1.3 Vary Controller Disable Time

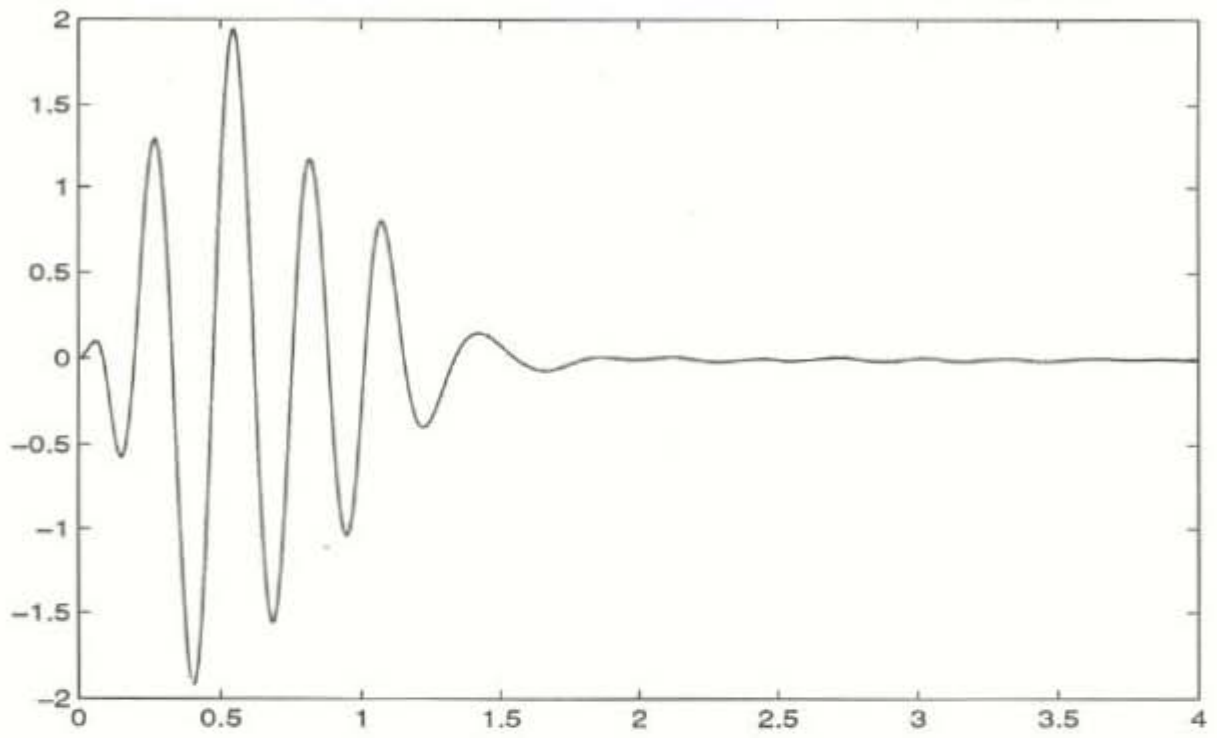
A different set of conditions are used in this section in order to demonstrate the optimal control parameters and their effect. The controller frequency is set at $\omega=16.3$ rad/s and the damping is $\zeta=0.05$ with the initial condition at 6 V. Here the disable time is varied by changing the time constant τ_d of a timing delay circuit, which cuts the output from the controller after the time constant expires. Figure 23 shows the response with $\tau_d=.878$. This is too late and misses the energy minimum which results in left over oscillations slightly larger than at the minimum.

Figure 23: Plant Response $\omega=16.3$ rad/s and $\zeta=0.05$ and IC=6V and $\tau_d=.878$



The response is significantly improved in Figure 24 with $\tau_d=0.756$. The remnant oscillations are virtually eliminated and the beam is returned to complete rest in just over 1.5 seconds.

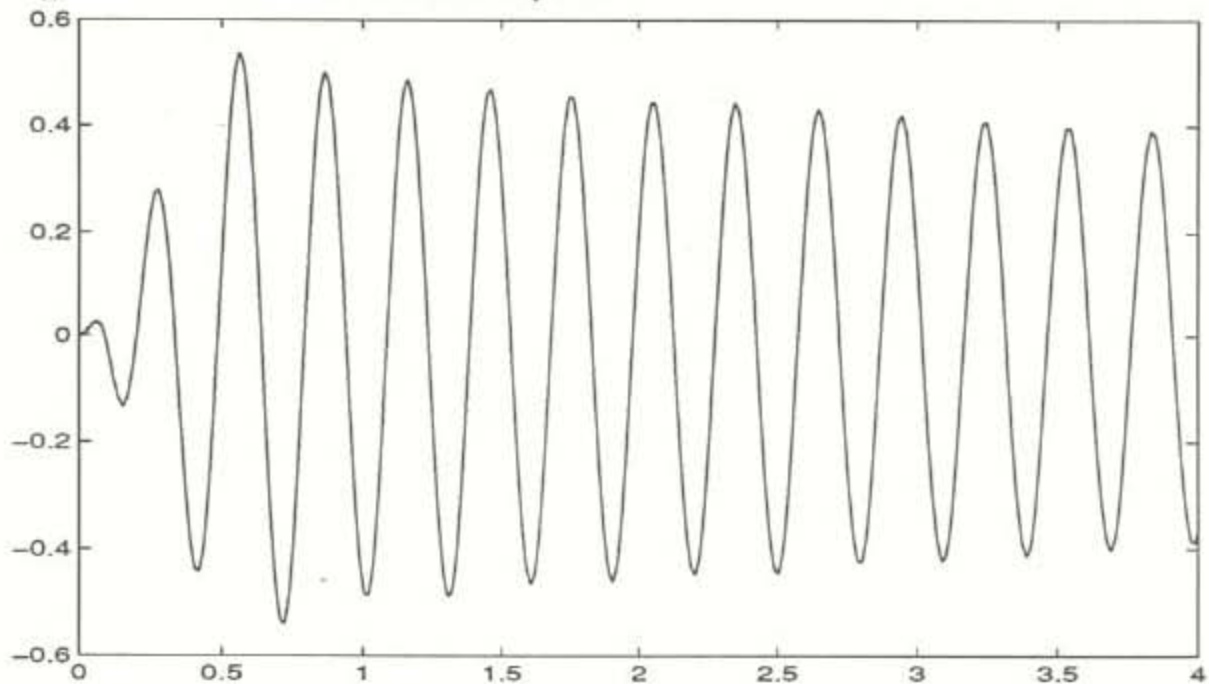
Figure 24: Plant Response $\omega=16.3$ rad/s and $\zeta=0.05$ and IC=6V and $\tau_d=0.756$



3.2 Beam Initial Position 11 mm

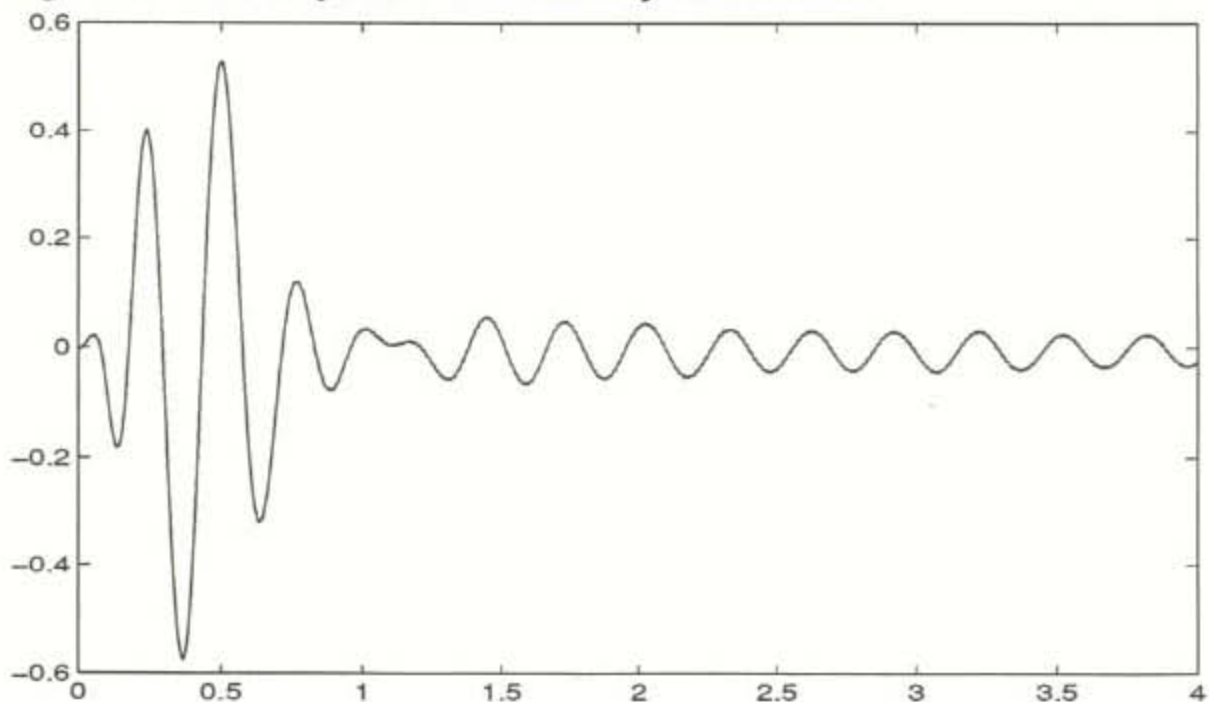
This initial condition when release without the controller enable requires approximately 30 seconds to come to rest, see Figure 25.

Figure 25: 11 mm Uncontrolled Response



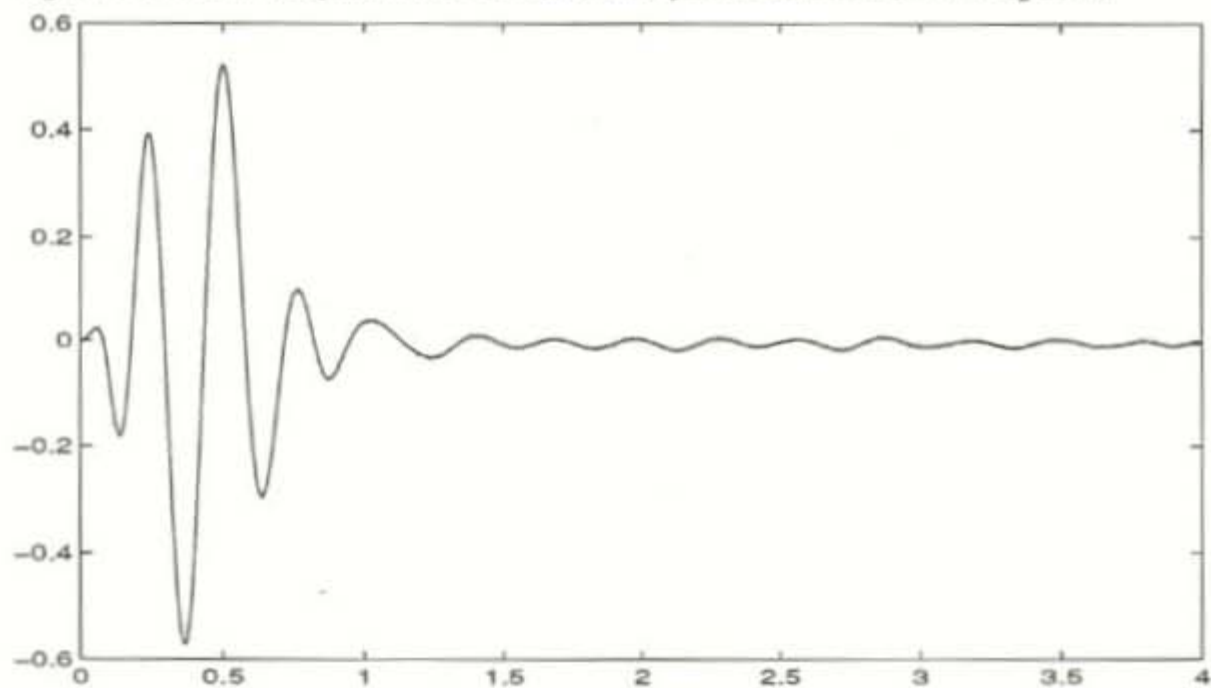
However, a dramatic improvement in the response is observed with the controller set for $\omega=19$ rad/s and $\zeta=0.3$ and IC=6V, however without the disable time operating, see Figure 26:

Figure 26: Plant Response $\omega=19$ rad/s and $\zeta=0.3$ and IC=6V



These leftover oscillations are eliminated with the disable time set at $\tau_d=.706$, and the resulting response lasts just over 1 second, see Figure 27.

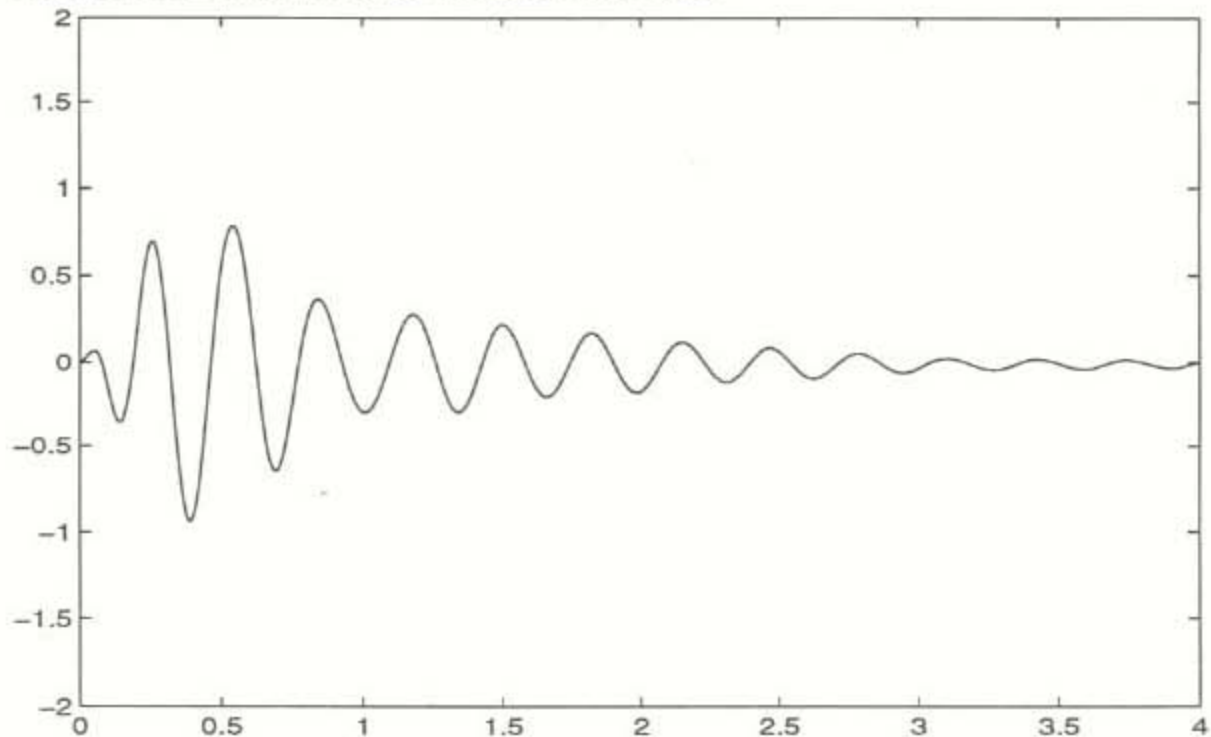
Figure 27: Plant Response $\omega=16.3$ rad/s and $\zeta=0.03$ and IC=6V and $\tau_d=.706$



3.3 Velocity Feedback Controller

Finally, a state feedback controller is also implemented [7], where negative velocity of the plant is used as the compensation signal to the piezoceramic elements. The result for the 29 mm initial condition is shown in Figure 28.

Figure 28: 29 mm with State Feedback Controller



It is clear that an acceptable response with decay time less than 3 seconds is obtained with this controller. However it must be noted that the state feedback controller cannot be tuned to eliminate oscillations completely as shown in Figure 27. Here the observation may be stated that the LC controller results in a cosine envelope for the response, which cannot be reproduced with the exponential decay envelope of a state feedback controller.

One advantage that the classical controller has over the LC controller is robustness. The classical controller is able to respond to any random input, ie any initial condition given anytime. The LC controller achieves results only when all initial parameters are known, and the first minimum has been established. Thus, there is a requirement for further enhancements to the LC controller which will allow it to respond to such random inputs. This will no doubt require some sort of computational algorithm which will assess initial parameters and automatically tune the controller accordingly.

4.0 Adaptation to Digital Control

As alluded to in the previous section, this type of controller may be enhanced by automating the parameter settings. In other words, the controller currently highly dependent on initial parameter values. Particularly the initial controller conditions do not necessarily perform the same for different initial plant positions. Furthermore, optimal controller frequency and damping are different for various initial plant conditions. Hence, it is necessary to include some sort of logical distinction between which control settings will be used at which times. A computer algorithm would lend itself well to such a scenario.

The first requirement would be an analog to digital converter capable of handling the frequency associated with the beam. The beam and control natural frequencies are on the order of 3 to 4 Hz, thus the A/D converter should be chosen to provide at least 100 points per cycle. The data stream collected from the plant would be discretized values of acceleration. These data may be integrated digitally via some forward or backward difference operation resulting in velocity and position information.

The goal of the algorithm would be to detect a variation from a standard set of bounds for the beam position, such that when the beam is disturbed beyond a certain tolerance limit, the control is enabled. Such limits may be set as small as desired. The magnitude of the deviation from the tolerance would then dictate the set of parameters which would return the plant to set point most efficiently. For large disturbances, low frequency and low damping would result in a similar response to that of the 29 mm initial condition, for small disturbances higher frequency and higher damping would be necessary. These values could be changed on the analog circuit by means of a digital to analog converter which would set the analog gains on the circuit corresponding to the digital values determined by the computer. Hence, it is not necessary to convert the entire controller to digital, only the portions where gains are set need be converted.

The continuous data stream would also prove useful for implementing the controller disable. Having full position data, it would be a matter of choosing a disable time coincident with the minimum of the position data. This could be predicted by means of an extrapolation algorithm that would predict minimum position and estimate at what time the disable should take place.

Thus, there is the potential for converting the LC controller to a more robust system capable of suppressing vibration in a plant with random inputs.

REFERENCES

- [1] Golnaraghi, M.F., "Dynamics & Control", Kluener Academic Publishers, 1991
- [2] Golnaraghi, M. F., "Vibration Suppression of Flexible Structures Using Internal Resonance", Pergamon Press, 1991
- [3] Duquette, A. P., "An Experimental Study of Vibration Control of a Flexible Beam via Modal and Co-ordinate Coupling", University of Waterloo, M.A.Sc. Thesis, 1991
- [4] Sensor Technology Ltd & BM Hi Tech, Product Brochure
- [5] Inman, D. J. "Engineering Vibrations", Prentice Hall, 1994
- [6] Thompson, W. T. "Theory of Vibration with Applications", Prentice Hall, 1988
- [7] Salemi, P "An Experimental Investigation and Finite Element Simulation of Piezoceramic Control of a Flexible Cantilever Beam", University of Waterloo, M.A.Sc. report.